

# Thermodynamic Analysis of the Biomass-to-Synthetic Natural Gas Using Chemical Looping Technology with CaO Sorbent

Haiming Gu,<sup>†</sup> Guohui Song,<sup>†</sup> Jun Xiao,<sup>†</sup> Hao Zhao,<sup>‡</sup> and Laihong Shen<sup>\*,†</sup>

<sup>†</sup>Key Laboratory of Energy Thermal Conversion and Control of Ministry of Education, School of Energy and Environment, Southeast University, Nanjing, 210096, People's Republic of China

<sup>‡</sup>Department of Mechanical and Aerospace Engineering, Princeton University, Princeton, New Jersey 08544, United States

**ABSTRACT:** This study evaluates the biomass-to-synthetic natural gas (SNG) using calcium looping gasification (CLG) with CaO sorbent (CLG-SNG) via thermochemical methods. The CLG-SNG process consists of three steps in sequence: steam gasification in situ CO<sub>2</sub> capture using CaO sorbents, gas cleaning, and methanation. The concept of interconnected fluidized beds was adopted for repeated carbonation/calcination cycles of CaO sorbents in the gasification unit. A process simulation was conducted based on the chemical equilibrium method using Aspen Plus. Then, the effects of some key variables on the thermodynamic performances, such as the gas composition, yield of SNG ( $Y_{\text{SNG}}$ ), cold gas efficiency ( $\eta_{\text{cold}}$ ), the overall energy efficiency ( $\eta$ ), exergy efficiency ( $\psi$ ) of the process, and the unit power consumption ( $W_{\text{SNG}}$ ) were investigated. The variables include CaO-to-biomass ratio (Ca/B) in the range of 0.7–1, steam-to-biomass ratio (S/B) in the range of 0.1–1.5, and gasification temperature ( $t_G$ ) in the range of 600–700 °C. At Ca/B = 0.83, i.e., a stoichiometric number of SN = 1, the CH<sub>4</sub> content in SNG and  $W_{\text{SNG}}$  each reach the maximum while the  $Y_{\text{SNG}}$  reaches the minimum. With S/B increasing from 0.1 to 1.5, CH<sub>4</sub> content in SNG gradually decreases while  $W_{\text{SNG}}$  shows an increasing tendency.  $Y_{\text{SNG}}$ ,  $\eta_{\text{cold}}$ ,  $\eta$ , and  $\psi$  reach the maximum at S/B = 0.6 (i.e., when the gasifier reach the heat equilibrium). Generally, lower  $t_G$  values are favorable for the thermodynamic performances (mainly  $Y_{\text{SNG}}$  and  $\eta_{\text{cold}}$ ) of the CLG-SNG process. The optimal performances demonstrate that the CLG-SNG process has a strong competitiveness, compared to the traditional SNG production process.

## 1. INTRODUCTION

As a widely available renewable energy source, biomass is considered as a potential feedstock for alternative gaseous and liquid fuels. Among the candidates for liquid and gaseous synthetic fuels by biomass thermochemical processes, methane is one of the most promising options, since the synthesis reaction approaches chemical equilibrium and its conversion efficiency is high.<sup>1</sup> Several research institutes are developing biomass-to-synthetic natural gas (SNG) technology, including Energy Research Center of The Netherlands (ECN), Paul-Scherrer Institute (PSI) in Switzerland, Center for Solar Energy and Hydrogen Research Baden-Württemberg (ZSW) and Technische Universität München (TUM) in Germany, and National Institute of Clean-and-Low-Carbon Energy (NICE) in China, etc.<sup>2–5</sup>

From the current state-of-art, the biomass-to-SNG process via thermochemical process consists of four principal steps in sequence (Figure 1),<sup>2</sup> i.e., biomass gasification, gas cleaning, methanation and CO<sub>2</sub> removal. The first step is biomass gasification and steam is the preferential gasifying medium. The product gases mainly contain H<sub>2</sub>, CO, CO<sub>2</sub>, H<sub>2</sub>O, CH<sub>4</sub> and some higher hydrocarbons and impurities such as sulfur and chlorine species. Gas cleaning should be understood as unit

operations in which the impurities and catalyst poisons (such as tars, and nitrogen and sulfur compounds) are removed from the product gas.<sup>2</sup> Methanation is the subsequent unit consisting of the gas conditions and fuel synthesis of syngas. The stoichiometric ratio of the reactants H<sub>2</sub>/CO in syngas fed to the methanation unit should be 3 at least. However, the syngas from the biomass gasifier usually has a H<sub>2</sub>/CO ratio between 0.3 and 2, which is too low for a good yield of CH<sub>4</sub>. Via the water-gas shift (WGS) reaction, the H<sub>2</sub>/CO ratio can be adjusted by converting CO with H<sub>2</sub>O to CO<sub>2</sub> and additional H<sub>2</sub>. The fuel synthesis is a heterogeneously catalyzed process that converts CO and H<sub>2</sub> to CH<sub>4</sub> and H<sub>2</sub>O. CH<sub>4</sub> and CO<sub>2</sub> (~45 vol %) are two major species in crude SNG, i.e., the product of methanation unit.<sup>6</sup> In the final step, most CO<sub>2</sub> in the crude SNG is removed to meet the related requirements of grid gas. Physical absorption, pressure swing absorption, polymeric membranes, etc. are the applicable technologies for CO<sub>2</sub> removal from crude SNG.<sup>7</sup> Water removal after these four major steps is also necessary for upgrading the quality of the crude SNG.

Recently many studies have investigated suitable technologies and processes for SNG production from biomass.<sup>1,4,6–13</sup> Generally, previous studies have focused on two aspects:

- (i) Development of chemical conversion technologies, such as designs of biomass gasifiers and methanation reactors<sup>8,9</sup> and development of catalyst for methanation reactions.<sup>10</sup>

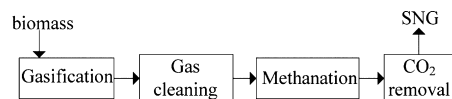


**Figure 1.** Block diagram of the traditional synthetic natural gas (SNG) process.

**Received:** December 4, 2012

**Revised:** July 14, 2013

**Published:** July 15, 2013

- (ii) Optimization of process conditions for both overall process and unit processes, such as temperatures and pressures in gasification and methanation reactors.<sup>6,7,11–14</sup>

Carbonation/calcination cycle of CaO sorbents is considered as an effective approach to capture CO<sub>2</sub> from flue gas at high temperatures. Abanades et al. carried out experiments in a pilot-scale fluidized bed reactor to investigate the carbonation reaction of CaO for CO<sub>2</sub> capture from combustion flue gases and observed high CO<sub>2</sub> capture efficiencies.<sup>15</sup> Carbonation/calcination cycle of CaO sorbents is also expected to enhance H<sub>2</sub> production from coal or biomass. Zhao et al. proposed a coal gasification process with in situ CO<sub>2</sub> capture using CaO sorbents capture via a three-stage system of interconnected fluidized beds.<sup>16</sup> In the case of gasification of Japanese oak, Hanaoka et al. found that, at a Ca/C molar ratio of  $\geq 1$ , CO<sub>2</sub> was not observed in the product gas any more.<sup>17</sup> Acharya et al. performed an experimental study to determine the potential of H<sub>2</sub> production from steam gasification of biomass in the presence of CaO and effects of operating parameters, such as S/B and Ca/B.<sup>18</sup> Florin and Harris presented a comprehensive review on enhanced H<sub>2</sub> production from biomass with in situ CO<sub>2</sub> capture using CaO sorbents. They reviewed the mechanism of in situ CO<sub>2</sub> capture using CaO, likely process operating configuration, optimization of reactor conditions, related operational challenges, as well as strategies for enhancing the multicycle reactivity of CaO, etc.<sup>19</sup>

The calcium-looping gasification (CLG) process of biomass could simultaneously improve H<sub>2</sub>/CO ratio and remove the CO<sub>2</sub> from the syngas. If the product gas with sufficiently low concentration of CO<sub>2</sub> and sufficiently high H<sub>2</sub>/CO ratio is used as feedstock for methanation unit, the CO<sub>2</sub> content in the crude SNG might be so low that the subsequent unit of CO<sub>2</sub> removal is not necessary. Acharya et al. compared different concepts of the CLG process for H<sub>2</sub>-rich gas production such as CO<sub>2</sub> acceptor process, HyPr-ring process, absorption enhanced reforming (AER) process, etc.<sup>20</sup> In the case of AER process, the concentrations of H<sub>2</sub>, CO, and CO<sub>2</sub> in the product gas are ~53%, ~17%, and ~12%, respectively.<sup>21</sup> On this basis, ZSW proposed a technical route of SNG production from the AER process.<sup>22</sup> As shown in Figure 2, the novel process comprises

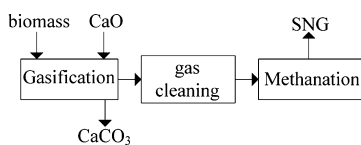


**Figure 2.** Block diagram of the process of biomass-to-synthetic natural gas via calcium-looping gasification (CLG-SNG), integrating biomass steam gasification with in situ CO<sub>2</sub> capture using CaO sorbents.

only three major steps, i.e., steam gasification of biomass coupled with in situ CO<sub>2</sub> capture using CaO sorbents, gas cleaning, and methanation. Compared with the traditional SNG, the present process does not involve an extra energy-intensive CO<sub>2</sub> removal unit and therefore, the related cost of investment and operation may be saved.

However, since ZSW proposed the SNG process integrating the AER process, no more investigation information on this topic can be found. The CLG-SNG is naturally subject to at least two doubts:

- (i) Can it can produce SNG with quality that matches that of natural gas?

- (ii) Can it can compete with the traditional process from the point of thermodynamic performances, such as the yield of SNG, energy, or exergy efficiencies?

To address the above-mentioned doubts, this study first specified a potential configuration of the CLG-SNG process. Subsequently, a simulation using Aspen Plus was performed. Then this study quantitatively investigated the feasibility and thermodynamic performances of the CLG-SNG process. The competitiveness of the novel process was demonstrated.

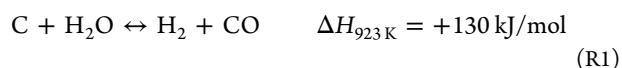
## 2. PROCESS CONFIGURATION AND MODELING

**2.1. Process Configuration.** Figure 3 graphically illustrates the specific configuration of the CLG-SNG process integrating steam gasification with in situ CO<sub>2</sub> capture using CaO sorbents. The process has three major steps, in the following sequence: (a) biomass steam gasification with carbonation/calcination cycle of CaO sorbents via interconnected fluidized beds (IFB), (b) hot gas cleaning, and (c) methanation via a single isothermal fluidized-bed methanation reactor (FBMR).

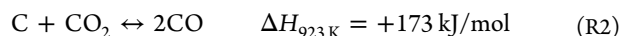
The prototype for biomass steam gasification with carbonation/calcination cycle of CaO sorbents is a system of interconnected fluidized beds constructed at Southeast University.<sup>23,24</sup> Briefly, it consists of a high-velocity fluidized bed as a combustor, a cyclone, a spout-fluid bed as a gasifier, and an inner seal. Through the cyclone and the seal, the CaO sorbent cycles between the two separated reactors.

In the gasifier, steam is designed to serve as the fluidizing gas for the bed materials (CaO sorbents) and the gasification medium for the biomass. As soon as biomass particles are fed to the gasifier, an exquisite contact among the biomass particles (BG), steam (SG), and high-temperature CaO sorbent occurs, followed by an intensive exchange of heat and mass. Biomass particles are rapidly heated to the bed temperature and gasified by steam to form a mixture of combustible gases. The main reactions involved could be described as follows:<sup>19</sup>

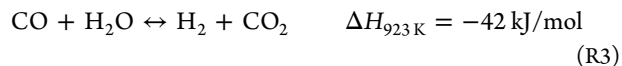
Heterogeneous water-gas shift:



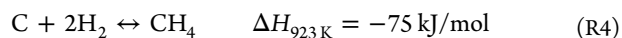
Boudouard equilibrium:



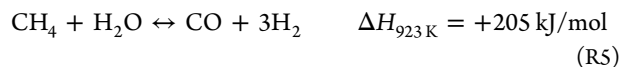
Water-gas shift (WGS):



Hydrogenating gasification:

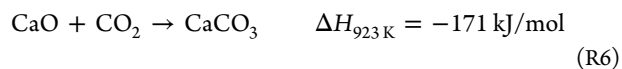


Methane reforming:



Reactions R1, R2, and R5 are intensive endothermic reactions, while reactions R3 and R4 are exothermic reactions. During the gasification process in the presence of CaO and CO<sub>2</sub> in the gaseous products is captured in the form of CaCO<sub>3</sub>:

Carbonation:



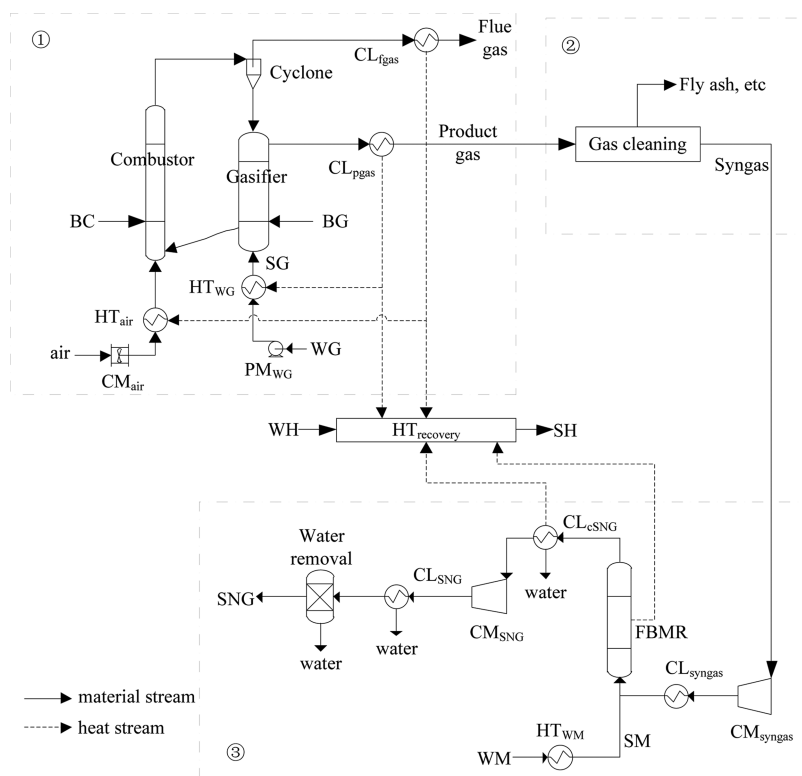
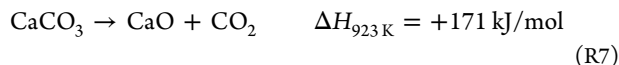


Figure 3. A specific configuration of the CLG-SNG process.

Reaction R6 has three advantages: (1)  $\text{CO}_2$  is captured; (2) the removal of  $\text{CO}_2$  alters the reaction equilibrium to induce reaction R3 to the right direction promoting the  $\text{H}_2/\text{CO}$  ratio, and (3) reaction R6 is an exothermic reaction that can compensate the heat needed in the gasifier.

By the gravitational force, the bed material is delivered through the inner seal to the combustor, which is fluidized by air. Before injected into the combustor, air is first compressed by a single-stage compressor  $\text{CM}_{\text{air}}$ , and then preheated to  $200\text{ }^\circ\text{C}$  by hot flue gas via a heater  $\text{HT}_{\text{air}}$  (Figure 3). Partial unreacted biomass char from the gasifier is delivered into the combustor along with the circulation bed materials. The biomass char is burnt out in the combustor releasing heat. A certain amount of biomass (BC) is usually utilized to totally satisfy the heat supply for gasification process and control the temperature in combustor. CaO sorbents are regenerated in the combustor according to the calcination reaction.

Calcination:



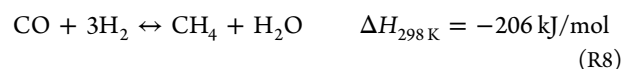
Reaction R7 is an intensive endothermic reaction, which consumes much of the heat released by biomass combustion. However, the energy used for calcination is recovered in the gasifier as mentioned. This characteristic of the IFB system could keep the energy and exergy efficiencies of the CLG-SNG process at reasonable and competitive levels. A test of long series of carbonation/calcination cycles of CaO sorbents shows that calcination temperatures over  $950\text{ }^\circ\text{C}$  and/or extended calcination times accelerate CaO sorbents degradation, reaching the residual capture capacity at a lower number of cycles.<sup>25</sup> Therefore, the temperature in combustor is kept at  $800\text{--}900\text{ }^\circ\text{C}$  in this study. The high-temperature bed materials are separated from flue gas through a cyclone separator, and then

they are introduced into a gasifier for a new cycle, while flue gas is exhausted from the top of the cyclone.

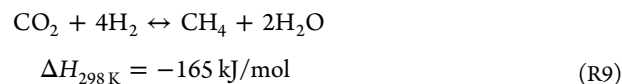
IFB physically separates the gasification and combustion processes in a gasifier and a combustor, respectively. Using IFB, the CaO sorbents allows repeated cycles of carbonation/calcination according to eqs 6 and 7. In addition, the gasifier produces a  $\text{H}_2$ -rich and almost  $\text{N}_2$ -free product gas, whereas the combustor produces a flue gas with relatively higher  $\text{CO}_2$  content. If a highly concentrated  $\text{CO}_2$  by-product is the key objective, pure  $\text{O}_2$  or indirect heating is preferable in order to avoid the dilution of a pure stream of  $\text{CO}_2$ . The later measure may involve three reactors.<sup>26</sup>

After gasification, high-temperature product gas is cooled by a cooler ( $\text{CL}_{\text{pgas}}$ ), and partial water may be removed by condensation as needed. Then, product gas is purified by hot gas cleaning technology, which integrates particle removal with candle filters or electrostatic precipitators, thermal or catalytic cracking of the tars, and high-temperature adsorption of other contaminants.<sup>7</sup>

Syngas prior to the compressor with intercooling ( $\text{CM}_{\text{sgas}}$ ) was cooled to  $70\text{ }^\circ\text{C}$ . Since high pressure is favorable to the methanation reactions, syngas (i.e., the product of the gas cleaning unit) is compressed by a single-stage or multistage compressor  $\text{CM}_{\text{sgas}}$  prior to the methanation unit (see Figure 3). In the methanation reactor, CO with  $\text{H}_2$  is converted to  $\text{CH}_4$ :



Depending on the initial syngas composition,  $\text{CO}_2$  with  $\text{H}_2$  might also be converted to  $\text{CH}_4$ :



The stoichiometric coefficients of reactions R8 and R9 allow one to determine the amount of hydrogen needed to completely reform CO and CO<sub>2</sub> to CH<sub>4</sub>. Thus, it is convenient to define the stoichiometric number (SN) of the incoming gas to characterize the achievable methane yield,<sup>7</sup> i.e.,

$$SN = \frac{x_{H_2}}{3x_{CO} + 4x_{CO_2}} \quad (1)$$

where  $x_{H_2}$ ,  $x_{CO}$ , and  $x_{CO_2}$  are the molar fractions of H<sub>2</sub>, CO, and CO<sub>2</sub> in the syngas, respectively. To obtain a highly pure methane stream, SN should be close to 1.

Methane synthesis from a H<sub>2</sub>/CO/CO<sub>2</sub> mixture is highly exothermic and its reactor design is critical with regard to temperature control. Methanation is expected to be carried out in a series of adiabatic fixed-bed reactors with intercooling and optional product recycle, or in a single isothermal once-through fluidized-bed reactor (FBMR).<sup>11</sup> FBMR allows for simultaneous methanation and WGS reactions in the presence of ethylene, which may exist in different syngas compositions without additional gas conditioning. Furthermore, long-term experiments showed that the fluidized methanation catalyst allowed for constantly high CO conversion (~98%).<sup>9</sup> Hence, FBMR is adopted in this process configuration.

After methanation, SNG is cooled by CM<sub>SNG</sub> and compressed by CM<sub>SNG</sub> (Figure 3) to ambient temperature, and partial water in SNG is removed by condensation to improve its quality.

**2.2. Process Modeling.** Varieties of biomass can be used for SNG production, e.g., wood, municipal solid waste, sludge, and straw. China is short of forest resources, but rich in agricultural residuals (mainly straw, wheat straw, corn stalk), which could be utilized for power generation. Thus, straw is used as the feedstock for SNG production in this study. The proximate and ultimate analyses, as well as higher heating value (HHV) of the straw, are listed in Table 1. According to several biomass power plants in

**Table 1. Composition of Straw**

composition	value
moisture (wt %, ar)	9.10
ash (wt %, db)	11.51
C (wt %, db)	38.91
H (wt %, db)	5.30
N (wt %, db)	1.06
S (wt %, db)	0.15
O (wt %, db)	43.07
high heating value, HHV (MJ/kg, ar)	15.1

Jiangsu Province, China, the feedstock of the biomass plants varies in the range of 26–46 t/h. Therefore, the present simulation is calculated with 30 t/h straw, corresponding to the scale of 126 MW<sub>th</sub> fuel input.

Generally, there are two categories of models for the simulation of a chemical process: (a) equilibrium models and (b) kinetic models. Based on the concept of Gibbs free-energy minimization, the equilibrium model does not consider the reactor size and it is already used for the simulation of biomass gasification.<sup>18,27</sup> It is favorable for identifying the maximum possible conversion of biomass and the theoretical efficiency. It is applicable to investigate the feasibility and optimal thermodynamic performances of the CLG-SNG process, which is the focus of this study. Further investigations are not worthwhile if the

CLG-SNG process is infeasible or its optimal performances could not compete with the traditional process.

Compared with experimental data, H<sub>2</sub> content from simulation based on equilibrium model is usually higher while CH<sub>4</sub> content is often lower. To obtain the simulation data close to the experiments, the present simulation of gasification is based on the RGibbs model with temperature correction. The property method is based on PR-BM model, and the property method of the steam in the steam generation is based on STEAMNBS model. The simulation of CLG-SNG process was based on the following assumptions and specifications:

(1) The contaminations in the biomass gasification products mainly contain HCN, NH<sub>3</sub>, H<sub>2</sub>S, COS, etc.<sup>28</sup> Actually, sorbents deactivation may be caused by the potential CaSO<sub>4</sub> formation.<sup>26</sup> However, as biomass contains a small amount of sulfur, influences of sulfide on CaO sorbents are neglected in this primary study, so we can focus on the objective of this study.

(2) The simulation of the circulation of CaO sorbent in the dual fluidized bed is realized by the method of “tear stream” by Aspen Plus. The function of “inert” could simulate deactivated CaO sorbent.

(3) Tar was not taken into account, because of the fact that CaO can break the tar and char into gaseous matter.<sup>18,27,29</sup>

(4) The reactors are operated under a steady state, and the residence time is long enough for the reactions to achieve chemical and phase equilibriums.

(5) Heat loss in IFB is taken as 3% of the total heat input, and the pressure losses in the reactors are assumed to 3 kPa.<sup>27</sup>

(6) The excess air number is set to 1.5 as a constant.<sup>27</sup>

(7) The energy balance of the IFB system is realized by a modified design specification based on Aspen Plus program.<sup>16,27</sup>

(8) The temperature of the product gas after the cooler is 400 °C. The pressure drop over the gas cleaning is assumed to be 0.2 bar, referring to that of dust removal in a power plant.<sup>30</sup>

(9) The pressure drop of the methanation reactor is taken as 0.5 bar.<sup>11</sup> The pressure of the syngas introduced to the methanation reactor is set at 10.5 bar, to ensure that the SNG pressure is 10 bar. FBMR is modeled to be operated at a constant temperature of 300 °C. The inlet pressure for the methanation reactor could be as low as 2.5 bar.<sup>11</sup> In this study, the methanation pressure is kept at 10 bar to guarantee good CO conversion.

(10) Designing a calcium-looping gasification reactor that operates at high temperature and pressure is challenging, and the continuous flow of solids among different pressurized reactors is even more difficult.<sup>20</sup> Therefore, the present gasification system is simulated at atmospheric pressure and relatively low temperature (600–700 °C).<sup>20</sup>

Several previous studies have demonstrated that heat recovery is significantly favorable to improve the overall energy and exergy efficiencies of a biomass-to-SNG process.<sup>4,7,13</sup> In this study, the excrescent sensible heat is recovered by cooling product gas, flue gas, and FBMR.

### 3. PERFORMANCE ASSESSMENT

To evaluate the novel process, some thermodynamic performances were examined, including the composition of SNG, SNG yield, cold gas efficiency, energy and exergy efficiencies, and unit power consumption.

**3.1. Composition and Yield of SNG.** Composition of SNG should be first examined. However, there is no standard on composition of biomass-based SNG so far. The ranges of the species in SNG indicated in Table 2 are summarized from refs 6,

**Table 2. Reviewed Compositions of SNG**

composition	Min	Max
CH <sub>4</sub> (vol %)	79.7	96.1
CO (vol %)	0	0.6
CO <sub>2</sub> (vol %)	0.5	8.4
H <sub>2</sub> (vol %)	0	11.4
N <sub>2</sub> (vol %)	0.1	2.6

7, 13, and 14. From Table 2, there may be certain amounts of CO<sub>2</sub> and H<sub>2</sub> existing in the biomass-based SNG. In the following sections, a sample of SNG with a CO<sub>2</sub> content of ≤8 vol % and a H<sub>2</sub> content of ≤11 vol % is regarded as qualified. The content of the gas composition in the present paper is presented on a dry basis (denoted as db). The contents of the formations of high hydrocarbons (C<sub>2</sub> and C<sub>3</sub>) are negligible. Therefore, other hydrocarbons besides CH<sub>4</sub> are not graphically shown in the paper. Furthermore, drawing lessons from the experimental setting by Seemann et al.,<sup>9</sup> the mole flow rate of the water added into the methanation unit (WM) is set to 10% of that of the input syngas (ar), and the carbon deposition was not observed in the simulation results.

SNG yield ( $Y_{SNG}$ ) is defined as follows:

$$Y_{SNG} \text{ (Nm}^3\text{/kg)} = \frac{V_{SNG}}{m_{BG} + m_{BC}} \quad (2)$$

where  $V_{SNG}$  is the volume flow rate of SNG (corresponding to 20 °C and 101.325 kPa), where  $m_{BG}$  and  $m_{BC}$ , presented in units of kg/h, are the mass flow rates of biomass fed to the gasifier and the combustor, respectively.

**3.2. Energy and Exergy Analyses.** Energy and exergy analyses of the process were based on the mass and energy

balances obtained from Aspen Plus simulation results. The cold gas efficiency ( $\eta_{cold}$ ) of the straw-to-SNG process was defined as

$$\eta_{cold} \text{ (%) } = \frac{V_{SNG}LHV_{SNG}}{(m_{BG} + m_{BC})LHV_{biomass}} \times 100 \quad (3)$$

The overall energy efficiency ( $\eta$ ) based on LHV was defined as the ratio between useful energy output from the process and the necessary energy input to this process:

$$\eta = \frac{V_{SNG}LHV_{SNG} + H_{SH}}{(m_{BG} + m_{BC})LHV_{biomass} + W_{CM}} \quad (4)$$

where  $LHV_{SNG}$  is the lower heating value of SNG,  $H_{SH}$  the enthalpy flow rate of SH, and  $H_{SG}$  the enthalpy flow rate of the gasifying medium steam (SG).  $LHV_{biomass}$  has been given in Table 1.  $P_{CM}$  is the total power consumption rate of all compressors involved in this presented process. The power consumption of a compressor was estimated with an assumption of isentropic efficiency of 0.8<sup>31</sup> and a mechanical efficiency of 0.98 for one single stage.

The exergy analysis was performed according to the method by Szargut et al.<sup>32</sup> Similarly, the overall exergy efficiency ( $\psi$ ) was defined as the ratio between the useful exergy output from the process and the necessary exergy input to this process:

$$\psi \text{ (%) } = \frac{Ex_{SNG} + Ex_{SH}}{\sum Ex_{IN} + W_{CM}} \times 100 \quad (5)$$

where  $Ex_{SNG}$  and  $Ex_{SH}$  are the exergy flow rates of SNG and steam generated by heat recovery (SH), respectively.  $\sum Ex_{IN}$  is the sum of the exergy flow rates of all entering material streams.

Exergy of a material stream ( $Ex$ ) includes two terms: physical exergy and chemical exergy. In the case of simulation using Aspen Plus software, the physical exergy of a conventional stream can be

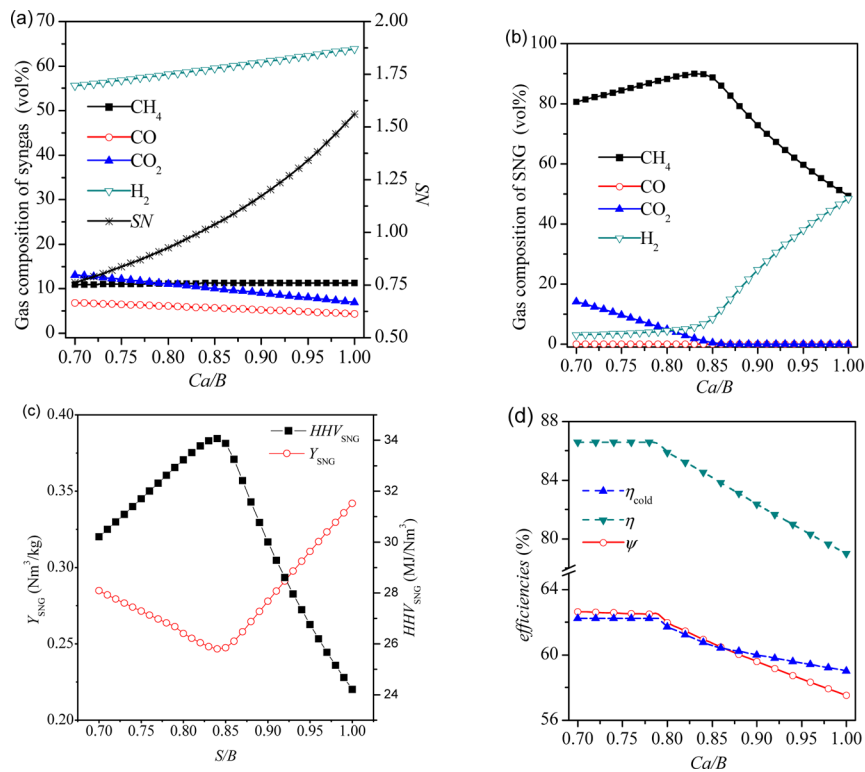


**Figure 4.** Effects of Ca/B on compositions of (a) syngas and (b) SNG, (c)  $Y_{SNG}$ , and the higher heating value ( $HHV_{SNG}$ ) and (d)  $\eta_{cold}$ ,  $\eta$ , and  $\psi$ , respectively.

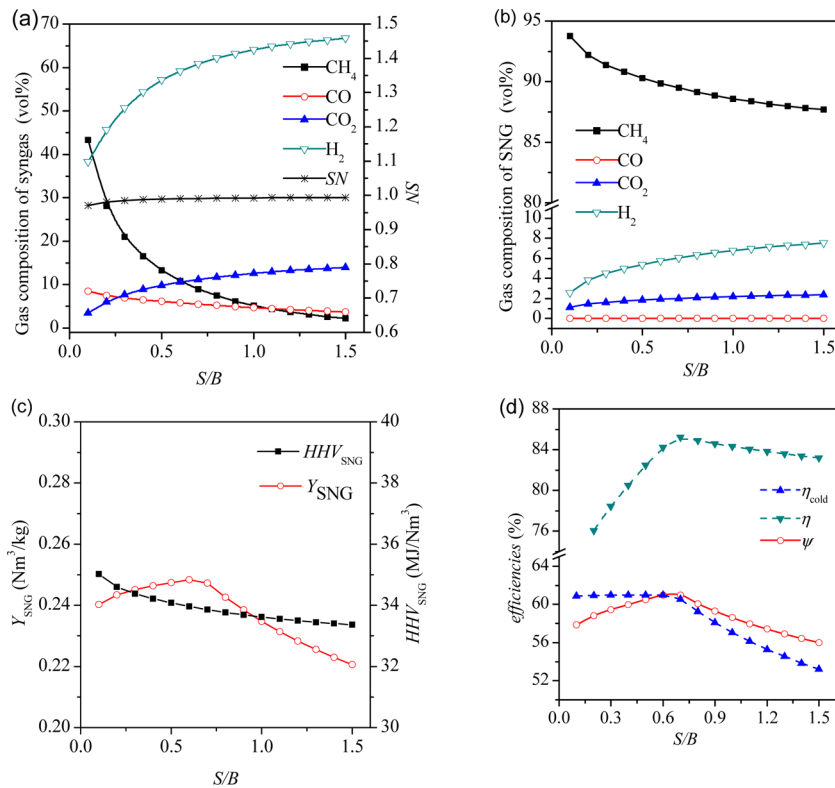


**Figure 5.** Effects of S/B on compositions of (a) syngas and (b) SNG and, (c)  $Y_{\text{SNG}}$  and  $\text{HHV}_{\text{SNG}}$ , and (d)  $\eta_{\text{cold}}$ ,  $\eta$ , and  $\psi$ , respectively.

calculated by calling the property AVAILMX in the Aspen Plus program. The chemical exergy of a stream was calculated based on Szargut's reference environmental model.<sup>33</sup>

With regard to the calculation of chemical exergy of biomass, the unified correlation for estimating the specific chemical exergy of solid and liquid fuels on a dry basis ( $e_{\text{ch,db}}$ ) was applied:<sup>34</sup>

$$e_{\text{ch,db}} \text{ (kJ/kg)} = 363.439C + 1075.633H - 86.308O + 4.147N + 190.798S - 21.1A \quad (6)$$

where  $C$ ,  $H$ ,  $O$ ,  $N$ , and  $S$  represent the weight percentages of elemental carbon, hydrogen, oxygen, nitrogen, and sulfur, on a dry basis, respectively;  $A$  is the weight percentage of ash on a dry basis.

**3.3. Unit Power Consumption.** It is clear from the process configuration that partial biomass fed into the system serves as the raw material for SNG production and the other part of biomass as well as power consumption serves as the driving force to produce SNG. Unit power consumption  $W_{\text{SNG}}$  could be used to characterize the power consumption during the SNG process.  $W_{\text{SNG}}$  is defined as the power consumption  $P_{\text{sum}}$  needed to produce 1 N m<sup>3</sup> of SNG.

$$W_{\text{SNG}} \text{ (kWh/Nm}^3\text{)} = \frac{P_{\text{sum}}}{V_{\text{SNG}}} \quad (7)$$

**3.4. Process Variables.** The influence of steam-to-biomass mass ratio (S/B), CaO-to-biomass mass ratio (Ca/B), and gasification temperature ( $t_{\text{G}}$ ) on the thermodynamic performances were studied.

S/B and Ca/B are defined as follows, respectively:

$$S/B = \frac{m_{\text{SG}}}{m_{\text{BG}}} \quad (8)$$

$$\text{Ca/B} = \frac{m_{\text{CaO}}}{m_{\text{BG}}} \quad (9)$$

where  $m_{\text{SG}}$  is the mass flow rates of the gasifying medium steam (SG) added into the gasifier.  $m_{\text{CaO}}$  is the circulation flow rate of CaO sorbents in IFB. The CaO sorbents here mean the fresh sorbents with the theoretical activity and, therefore, we can focus on the feasibility and optimal process performances of the CLG-SNG process.

## 4. RESULTS AND DISCUSSIONS

In this section, the standard process conditions in simulations were as follows: S/B = 0.584, Ca/B = 0.83,  $t_{\text{G}} = 650$  °C,  $\Delta t_{\text{IFB}} = 200$  °C,  $p_{\text{G}} = 1$  bar,  $t_{\text{air}} = 100$  °C,  $p_{\text{air}} = 1$  bar,  $t_{\text{SG}} = 300$  °C,  $p_{\text{SG}} = 1$  bar,  $t_{\text{M}} = 300$  °C,  $p_{\text{M}} = 10$  bar,  $t_{\text{WM}} = 300$  °C,  $p_{\text{WM}} = 10.5$  bar. In the subsequent process simulations, one of these parameters varied while the remaining parameters were kept constant.

**4.1. Effect of Ca/B.** In the present CLG-SNG process, the CaO sorbents are utilized to capture CO<sub>2</sub> from the syngas, which can promote the WGS reaction to a higher H<sub>2</sub> content and a lower CO content in the syngas. When the Ca/B increases from 0.7 to 1.0, the H<sub>2</sub> content in syngas gradually increases from 55.6 vol % to 63.9 vol %, while CO<sub>2</sub> content decreases slightly (Figure 4a). Correspondingly, SN rises from 0.76 to 1.56, and is equal to 1 at Ca/B = 0.83.

Figure 4b indicates that the composition of SNG is sensitive to Ca/B. When Ca/B < 0.83 (i.e., SN < 1), the amount of H<sub>2</sub> is not enough to convert all CO and CO<sub>2</sub> in the following methanation unit. In this case, with increasing Ca/B, the H<sub>2</sub> content in the SNG remains very low, while CO<sub>2</sub> content gradually decreases (Figure 4b). When Ca/B ≥ 0.83 (i.e., SN ≥ 1), the amount of H<sub>2</sub> is redundant to convert CO and CO<sub>2</sub> to CH<sub>4</sub> in the methanation unit. In this case, with increasing Ca/B, the contents of CO and CO<sub>2</sub> remain very low, while the H<sub>2</sub> content in the SNG gradually

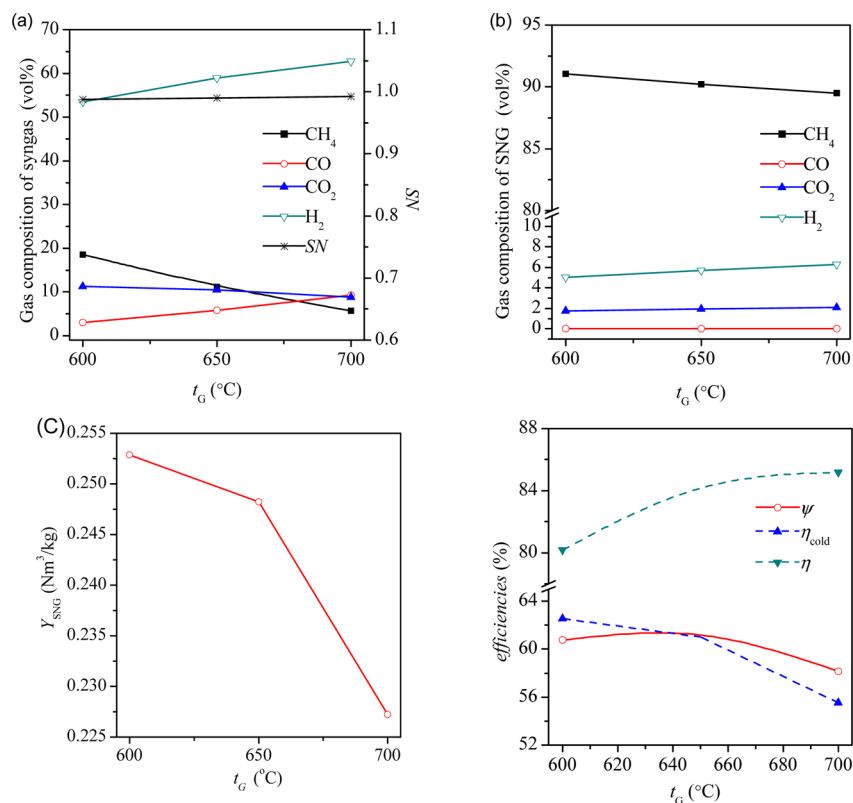


**Figure 6.** Effects of  $t_G$  on compositions of (a) syngas and (b) SNG, (c)  $Y_{\text{SNG}}$ , and (d)  $\eta_{\text{cold}}$ ,  $\eta$ , and  $\psi$ , respectively.

increases, which further leads to the decrease in  $\text{CH}_4$  content (see Figure 4b). Over the entire Ca/B range of 0.7–1.0, the  $\text{CH}_4$  content reaches the maximum of 89.9 vol % at Ca/B = 0.83, i.e., SN = 1. To meet Chinese technical standard requirements for the HHV of natural gas, the proper Ca/B for straw is within the range of 0.74–0.88.

When Ca/B increases from 0.7 to 1.0,  $Y_{\text{SNG}}$  first decreases monotonously and then increases (Figure 4c), which has an opposite tendency, compared with the  $\text{CH}_4$  content in SNG. Note that, although  $Y_{\text{SNG}}$  is attractive when Ca/B < 0.74 or Ca/B > 0.88, the composition of SNG is not qualified anymore, according to Table 2. Under the above-mentioned process conditions,  $Y_{\text{SNG}}$  with qualified composition approximately varies in the interval of 0.247–0.274 N m<sup>3</sup>/kg. In addition, when Ca/B > 0.83, the  $\text{H}_2$  content increases rapidly and it is unfavorable for the transport and utilization of SNG. Therefore, a lower Ca/B should be given priority consideration over a larger  $Y_{\text{SNG}}$ . Since  $\text{CH}_4$  with an HHV value is the main composition of SNG, as shown in Figure 4c, the HHV<sub>SNG</sub> retains the same trend with  $\text{CH}_4$  content in SNG.

Both energy and exergy flow rates of SNG decrease very slightly over the entire Ca/B range. The variations of the efficiencies ( $\eta_{\text{cold}}$ ,  $\eta$ , and  $\psi$ ), are mainly dominated by the variation of  $m_{\text{BC}}$ . Figure 4d shows that the efficiencies changes little over the Ca/B range of 0.7–0.78. When Ca/B ≤ 0.78, the heat released by the carbonation reaction is less than that required by the gasification process. In this case, mainly depending on the heat required by the gasification process,  $m_{\text{BC}}$  changes little and, correspondingly,  $\eta_{\text{cold}}$ ,  $\eta$ , and  $\psi$  remain almost unchanged. However, when Ca/B > 0.78, the heat released by the carbonation reaction is greater than that required by the gasification process. In this case,  $m_{\text{BC}}$  linearly increases as Ca/B increases, which further leads to the decrease in the

efficiencies (Figure 4d). In addition, with increasing Ca/B,  $W_{\text{SNG}}$  first slowly increases and then rapidly decreases, and reaches the maximum of 0.621 kWh/Nm<sup>3</sup> at Ca/B = 0.83.

**4.2. Effect of S/B.** An increase in the amount of steam added into the gasifier would enhance reactions R1 and R3, which results in higher  $\text{H}_2$  and  $\text{CO}_2$  contents but a lower CO content in the syngas (Figure 5a). It is interesting that, within the range of 0.1–1.5, S/B has a negligible effect on SN, which remains almost unchanged at 0.99. However, from Figure 5b, the CO content in SNG is nearly zero while both the  $\text{H}_2$  and  $\text{CO}_2$  contents in SNG increase with increasing S/B. It could be ascribed to reaction R6, which is promoted in the backward direction, because of a higher  $\text{H}_2\text{O}$  content. Finally, a lower  $\text{CH}_4$  content in SNG is obtained at a higher S/B. Regardless, the composition of SNG could satisfy the requirements listed in Table 2.

According to Figures 5b and 5c, the HHV<sub>SNG</sub> shows the same trend with  $\text{CH}_4$  content in SNG.  $Y_{\text{SNG}}$  first increases and then decreases over the S/B range of 0.1–1.5.  $Y_{\text{SNG}}$  approximately varies between 0.221 Nm<sup>3</sup>/kg and 0.248 Nm<sup>3</sup>/kg, and reaches a maximum at S/B = 0.6. As mentioned above, the calcination of  $\text{CaCO}_3$  in the combustor would release heat, which could be used as heat compensation for the endothermic gasification process. When S/B < 0.6, the circulation rate of CaO sorbent (exothermic reaction R6) absolutely satisfies the heat requirement for the gasification process. It means that the cooling of the gasifier is necessary to maintain the given gasification temperature and no extra  $m_{\text{BC}}$  is needed when S/B increases from 0.1 to 0.6. Therefore,  $Y_{\text{SNG}}$  is mainly affected by  $V_{\text{SNG}}$ , according to eq 2. Larger  $m_{\text{SG}}$  would promote reactions R1 and R5 and then cause a larger flow of SNG, which finally leads to a larger  $Y_{\text{SNG}}$ . In contrast, when S/B > 0.6, extra  $m_{\text{BC}}$  should be provided to supply the extra heat for the gasification process, which finally causes a rapid decrease in  $Y_{\text{SNG}}$ .

However, in a practical operation, because of the low contact efficiency between the steam and biomass and the short contact time needed to obtain reaction equilibrium, the S/B value should not be too low. Excess steam and even  $S/B > 1$  was suggested by Acharya.<sup>18</sup> A large S/B value is obviously unfavorable for the  $\text{CH}_4$  content and the  $Y_{\text{SNG}}$ . Furthermore, the elevated S/B would result in a lower  $\text{CO}_2$  partial pressure, and it is unfavorable for the capture of  $\text{CO}_2$ . Therefore, to experimentally determine a proper value of S/B based on the interconnected fluidized bed is meaningful for further experiment and simulation investigations.

As shown in Figure 5d, with the increase of S/B,  $\eta_{\text{cold}}$  first increases very slightly and then decreases sharply; similarly, both  $\eta$  and  $\psi$  first increase and then decrease obviously. These three efficiencies reach their maximum at  $S/B = 0.6$ , respectively. When S/B increases from 0.1 to 0.6,  $m_{\text{BC}}$  remains unchanged, which leads to a slight increase in  $\eta_{\text{cold}}$  (see eq 3). Meanwhile, the increase in  $m_{\text{SG}}$  causes a larger flow of syngas and SNG, which means more waste heat can be recovered. Therefore,  $\eta$  and  $\psi$  increase with S/B, according to eqs 4 and 5. However, in the case of  $S/B > 0.6$ ,  $m_{\text{BC}}$  linearly increases with S/B, which causes more exergy loss in both the combustor and the gasifier and, subsequently, the decrease in  $\eta_{\text{cold}}$ ,  $\eta$ , and  $\psi$ . In addition,  $W_{\text{SNG}}$  gradually increases with S/B in the interval of 0.1–1.5. The simulation result indicates that the power consumption of the related power equipment, especially the  $\text{CM}_{\text{syngas}}$ , would increase at a higher S/B and further result in a higher  $W_{\text{SNG}}$ .

**4.3. Effect of  $t_G$ .** Figure 6a shows the compositions of syngas and SNG in the  $t_G$  range of 600–700 °C. The  $\text{CO}_2$  content in syngas gradually decreases with  $t_G$ , while the  $\text{H}_2$  content has an opposite tendency.  $\text{CO}_2$  content in syngas is the combination result of the WGS reaction (reaction R3) and the carbonation reaction (reaction R6). The elevated temperature would promote these two exothermic reactions (i.e., reactions R6 and R3) to shift toward the backward direction.  $\text{CO}_2$  content in syngas should be dominated by carbonation reaction of CaO. Meanwhile, improving  $t_G$  would promote reactions R1, R2, and R5 to shift toward the forward direction, resulting in a continuous increase in CO content and a decrease in  $\text{CH}_4$  content in syngas.

Figure 6b indicates that no obvious indirect effect is observed between  $t_G$  and the composition of SNG. With increasing  $t_G$ , the  $\text{CH}_4$  content in SNG slightly decreases while the  $\text{H}_2$  content slightly increases. The contents of CO and  $\text{CO}_2$  in SNG remain almost unchanged at low values. However, as shown in Figure 6c, an obvious decrease in  $Y_{\text{SNG}}$  is observed, especially at  $t_G > 650$  °C. The net heat of the gasifier at 700 °C, rather than at 600 or 650 °C, is negative; this means that, at  $t_G = 700$  °C, more biomass ( $m_{\text{BC}}$ ) is fed to the combustor to compensate the heat requirement to maintain the temperature in the gasifier. Therefore, the slight decrease in  $Y_{\text{SNG}}$  at 650 °C is due to the lower production volume of SNG while the sharp decrease in  $Y_{\text{SNG}}$  at 700 °C is mainly dominated by the increase in  $m_{\text{BC}}$ . It seems that a lower  $t_G$  is favorable for the CLG-SNG process.

As shown in Figure 6d,  $\eta_{\text{cold}}$  gradually decrease with  $t_G$  while  $\eta$  gradually increase and  $\psi$  exhibits a tendency of first increase and then decrease trend. The large decrease in  $\eta_{\text{cold}}$  and  $\eta$  are ascribed to more biomass ( $m_{\text{BC}}$ ) fed to the combustor as mentioned above. The  $\eta_{\text{cold}}$ ,  $\eta$ , and  $\psi$  values remain at 62.5%–55.5%, 80.2%–85.2%, and 60.8%–58.1%, respectively. Furthermore,  $W_{\text{SNG}}$  gradually increase from 0.523 kWh/Nm<sup>3</sup> at 600 °C to 0.719 kWh/Nm<sup>3</sup> at 700 °C. From this point, lower  $t_G$  is a better choice. The above results indicate that, although a wider range of

gasification temperature is available, lower  $t_G$  should be preferentially chosen for this process.

In addition, the effect of  $\Delta t_{\text{IFB}}$  (i.e.,  $t_C - t_G$ ) on  $Y_{\text{SNG}}$ ,  $\eta$ ,  $\psi$ , and  $W_{\text{SNG}}$  is also investigated at  $t_G = 650$  °C. However, with  $\Delta t_{\text{IFB}}$  increasing from 150 °C to 250 °C (corresponding to  $t_C$  increasing from 800 °C to 900 °C), no obvious effect is observed.

#### 4.4. Competitiveness Analysis of the CLG-SNG Process.

To demonstrate the competitiveness of CLG-SNG production process, the performances of the process were compared with those of a traditional straw-to-SNG process, which mainly consists of four major units, i.e., biomass gasification via IFB with inert heat carrier as the bed material, hot gas cleaning, fluidized-bed methanation reactor, and selexol process for  $\text{CO}_2$  removal. The simulation parameters of the first three steps are the same with the CLG-SNG production processes. The simulation and energy performance assessment of the selexol process for  $\text{CO}_2$  removal has been reported in our previous work.<sup>35</sup> The final states of the product SNG by the two processes are the same and further water removal is also necessary for upgrading the quality of the crude SNG. Thus, the key process parameters for the maximum of  $C_{\text{CH}_4}$  or  $Y_{\text{SNG}}$ , as well as the corresponding performances of the two processes are presented in Table 3. The temperature and pressure of the methanation reaction are constants (300 °C and 10 bar, respectively).

**Table 3. Optimal Performances of the CLG-SNG Process and the Traditional SNG Process**

	Traditional SNG		CLG-SNG	
$t_G$ (°C)	750		600	
$t_C$ (°C)	825		800	
S/B	0.339		0.584	
$\alpha$	0.88	0.98		
Ca/B			0.74	0.83
SNG composition (vol %)				
CH <sub>4</sub>	84.05	92.14	84.48	91.04
CO	0.09	0.10	0.01	0.00
CO <sub>2</sub>	10.54	1.92	10.57	1.76
H <sub>2</sub>	3.30	3.62	2.93	5.00
HHV <sub>SNG</sub> (MJ/Nm <sup>3</sup> )	31.5	34.6	31.6	34.3
$Y_{\text{SNG}}$ (Nm <sup>3</sup> /kg)	0.303	0.276	0.314	0.286
$\eta_{\text{cold}}$	68.8	68.7	72.6	70.7
$\psi$ (%)	66.2	65.9	67.9	66.2
$\eta$ (%)	88.8	88.7	84.2	82.5
$W_{\text{SNG}}$ (kWh/Nm <sup>3</sup> )	0.779	0.856	0.466	0.495

The results on the both SNG production processes have shown that the option performance of these two SNG process have two contradictory directions: (1) the maximum of the  $\text{CH}_4$  content in SNG, and (2) the maximum yield of SNG. For example,  $C_{\text{CH}_4}$  increases but  $Y_{\text{SNG}}$  decreases with the  $\text{CO}_2$  removal efficiency ( $\alpha$ ) for the traditional process.  $C_{\text{CH}_4}$  also has a reverse trend to  $Y_{\text{SNG}}$  with variation of Ca/B for the CLG-SNG process (Figure 4). It seems that the two processes could obtain similar maxima for  $\text{CH}_4$  content and SNG yield with proper parameters. The maximum value of  $Y_{\text{SNG}}$  for the CLG-SNG (0.286–0.314 Nm<sup>3</sup>/kg) is slightly higher than that for traditional SNG (0.276–0.303 Nm<sup>3</sup>/kg). The  $\eta_{\text{cold}}$  value of the CLG-SNG (72.6%–70.7%) is slightly higher than the traditional SNG (68.7%–68.8%), and it indicates a higher utilization efficiency of the biomass for the CLG-SNG.



The exergy efficiency of the CLG-SNG process is slightly higher than that of the traditional SNG process, while the energy efficiency is slightly lower. Furthermore, from Table 3, there is an obvious difference in  $W_{\text{SNG}}$  between the two processes.  $W_{\text{SNG}}$  for the CLG-SNG process (0.466–0.495 kWh/Nm<sup>3</sup>) is much lower than that for the traditional SNG (0.779–0.856 kWh/Nm<sup>3</sup>). It is a potential significant advantage for the CLG-SNG process. To summarize, this implies that the CLG-SNG process has an attractive competitiveness, compared to the traditional SNG production process, judging from the thermodynamic performances.

## 5. CONCLUSIONS

The biomass-to-synthetic natural gas (SNG) using calcium looping gasification (CLG) (CLG-SNG) process consists of three major steps, i.e., biomass steam gasification with in situ CO<sub>2</sub> capture using CaO sorbents (CLG), gas cleaning, and methanation. A specific configuration of the CLG-SNG process unit using IFB for gasification was designed. The IFB allows repeated of carbonation/calcination cycles of CaO sorbents, realizing in situ CO<sub>2</sub> capture. Compared with traditional biomass-to-SNG process, the presented process does not involve the CO<sub>2</sub> removal unit.

To determine the feasibility and competitiveness of the CLG-SNG process, the thermodynamic performances, including the composition of SNG,  $Y_{\text{SNG}}$ ,  $\eta_{\text{cold}}$ ,  $\eta$ ,  $\psi$ , and  $W_{\text{SNG}}$  were the subjects of focus. The effects of some key variables, including a calcium-to-biomass ratio (Ca/B) in the range of 0.7–1, a steam-to-biomass ratio (S/B) in the range of 0.1–1.5, and gasification temperature ( $t_{\text{G}}$ ) in the range of 600–700 °C were investigated. The results show that the SNG composition is sensitive to Ca/B, and the proper Ca/B varies between 0.74 and 0.88 for the straw used in this study. At Ca/B = 0.83 (i.e., SN = 1), the CH<sub>4</sub> content in the SNG and the unit power consumption reach maximum values while the  $Y_{\text{SNG}}$  reaches the minimum value. With S/B increasing from 0.1 to 1.5, the CH<sub>4</sub> content gradually decreases while  $W_{\text{SNG}}$  shows an increasing tendency.  $Y_{\text{SNG}}$ ,  $\eta_{\text{cold}}$ ,  $\eta$ , and  $\psi$  reach the maxima at S/B = 0.6 (i.e., when the gasifier reaches the heat equilibrium). Generally, a lower  $t_{\text{G}}$  value is favorable for the thermodynamic performances (mainly  $Y_{\text{SNG}}$  and  $\eta_{\text{cold}}$ ) of the novel process.

Guided by the above findings, the optimal values of  $Y_{\text{SNG}}$ ,  $\eta_{\text{cold}}$ ,  $\eta$ ,  $\psi$ , and  $W_{\text{SNG}}$  are 0.314 N m<sup>3</sup>/kg, 72.6%, 84.2%, 67.9%, and 0.466 kWh/Nm<sup>3</sup>, respectively. From the point of thermodynamic performances, the present CLG-SNG process could totally compete with the traditional process.

## AUTHOR INFORMATION

### Corresponding Author

\*Tel.: +86 25 83795598. Fax: +86 25 83793452. E-mail address: lhshen@seu.edu.cn.

### Notes

The authors declare no competing financial interest.

## ACKNOWLEDGMENTS

This work was financially supported by the Special Fund for Major State Basic Research Projects of China (Nos. 2010CB732206 and 2013CB228106), the National Natural Science Foundation of China (No. 51276037), the Key Technology Research and Development Program of Jiangsu Province of China (No. BE2012166), and the Scientific Research

Foundations of Graduate School of Southeast University (Nos. YBJJ1206 and YBJJ1219).

## NOMENCLATURE

### Abbreviations

ar = as-received basis  
 BC = biomass fed to combustor  
 BG = biomass fed to gasifier  
 CL = cooler  
 CM = compressor  
 db = dry basis  
 Ex = exergy  
 FBMR = isothermal fluidized bed methanation reactor  
 HT = heater  
 IFB = interconnected fluidized bed  
 S/B = steam-to-biomass ratio  
 SG = steam fed to gasifier  
 SH = steam generated by heat recovery  
 SN = stoichiometric number  
 SNG = synthetic natural gas

### Variables

Ca/B = ratio of circulation flow rate of CaO to mass flow rate of biomass  
 $H$  = enthalpy  
 HHV = higher heating value  
 $m$  = mass flow rate  
 LHV = lower heating value  
 $p$  = pressure  
 $t$  = temperature  
 $V$  = volume flow rate  
 $P_{\text{CM}}$  = total power consumption rate  
 $W_{\text{SNG}}$  = unit power consumption  
 $x$  = molar fraction

### Greek Symbols

$\alpha$  = CO<sub>2</sub> removal efficiency  
 $\eta_{\text{cold}}$  = cold gas efficiency  
 $\eta$  = overall energy efficiency  
 $\psi$  = overall exergy efficiency

### Subscripts

G = gasifier  
 C = combustor  
 IN = input material stream

## REFERENCES

- Gassner, M.; Baciocchi, R.; Maréchal, F.; Mazzotti, M. Integrated design of a gas separation system for the upgrade of crude SNG with membranes. *Chem. Eng. Process.* **2009**, *48*, 1391–1404.
- Kopyscinski, J.; Schildhauer, T. J.; Biollaz, S. M. A. Production of synthetic natural gas (SNG) from coal and dry biomass—A technology review from 1950 to 2009. *Fuel* **2010**, *89*, 1763–1783.
- Fendt, A.; Tremel, A.; Gaderer, M.; Spliethoff, H. The potential of small-scale SNG production from biomass gasification. *Biomass Convers. Biorefin.* **2012**, *2*, 275–283.
- Tremel, A.; Gaderer, M.; Spliethoff, H. Small-scale production of synthetic natural gas by allothermal biomass gasification. *Int. J. Energy Res.* **2013**, *37* (11), 1318–1330.
- National Institute of Clean-and-low-carbon Energy. *Coal & Biomass to SNG* <http://www.nicenergy.com/> (accessed Oct. 16, 2012).
- Duret, A.; Friedli, C.; Maréchal, F. Process design of Synthetic Natural Gas (SNG) production using wood gasification. *J. Clean. Prod.* **2005**, *13*, 1434–1446.
- Gassner, M.; Maréchal, F. Thermo-economic process model for thermochemical production of Synthetic Natural Gas (SNG) from lignocellulosic biomass. *Biomass Bioenergy* **2009**, *33*, 1587–1604.

- (8) Gassner, M.; Maréchal, F. Thermodynamic comparison of the FICFB and Viking gasification concepts. *Energy* **2009**, *34*, 1744–1753.
- (9) Seemann, M. C.; Schildhauer, T. J.; Biollaz, S. M. A. Fluidized bed methanation of wood - derived producer gas for the production of synthetic natural gas. *Ind. Eng. Chem. Res.* **2010**, *49*, 7034–7038.
- (10) Struis, R. P. W. J.; Schildhauer, T. J.; Czekaj, I.; Janousch, M.; Biollaz, S. M. A.; Ludwig, C. Christian Ludwig. Sulphur poisoning of Ni catalysts in the SNG production from biomass: A TPO/XPS/XAS study. *Appl. Catal., A* **2009**, *362*, 121–128.
- (11) Heyne, S.; Seemann, M. C.; Harvey, S. Integration study for alternative methanation technologies for the production of synthetic natural gas from gasified biomass. *Chem. Eng. Trans.* **2010**, *21*, 409–414.
- (12) Heyne, S.; Seemann, M. C.; Harvey, S. Production of synthetic natural gas from biomass—process integrated drying. In *22nd International Conference on Efficiency, Cost, Optimization Simulation and Environmental Impact of Energy Systems*, ABCM, Foz do Iguaçu, Paraná, Brazil, 2009; pp 1877–1886.
- (13) Juraščík, M.; Sues, A.; Ptasiński, K. J. Exergy analysis of synthetic natural gas production method from biomass. *Energy* **2010**, *35*, 880–888.
- (14) Vitasari, C. R.; Jurascik, M.; Ptasiński, K. J. Exergy analysis of biomass-to-synthetic natural gas (SNG) process via indirect gasification of various biomass feedstock. *Energy* **2011**, *36*, 3825–3837.
- (15) Abanades, J. C.; Anthony, E. J.; Lu, D. Y.; Salvador, C.; Alvarez, D. Capture of CO<sub>2</sub> from combustion gases in a fluidized bed of CaO. *AIChE J.* **2004**, *50*, 1614–1622.
- (16) Zhao, H.; Song, G.; Shen, L.; Yu, Y. Novel Technique Route of Coal Gasification with CO<sub>2</sub> Capture Using CaO Sorbents via Three-Stage Interconnected Fluidized Beds. *Energy Fuels* **2012**, *26*, 2934–2941.
- (17) Hanaoka, T.; Yoshida, T.; Fujimoto, S.; Kamei, K.; Harada, M.; Suzuki, Y.; Hatanoc, H.; Yokoyama, S.; Minowaa, T. Hydrogen production from woody biomass by steam gasification using a CO<sub>2</sub> sorbent. *Biomass Bioenergy* **2005**, *28*, 63–68.
- (18) Acharya, B.; Dutta, A.; Basu, P. An investigation into steam gasification of biomass for hydrogen enriched gas production in presence of CaO. *Int. J. Hydrogen Energy* **2010**, *35*, 1582–1589.
- (19) Florin, N. H.; Harris, A. T. Enhanced hydrogen production from biomass with in situ carbon dioxide capture using calcium oxide sorbents. *Chem. Eng. Sci.* **2008**, *63*, 287–316.
- (20) Acharya, B.; Dutta, A.; Basu, P. Circulating-fluidized-bed-based calcium-looping gasifier: Experimental studies on the calcination–carbonation cycle. *Ind. Eng. Chem. Res.* **2012**, *51*, 8652–8660.
- (21) Koppatz, S.; Pfeifer, C.; Rauch, R.; Hofbauer, H.; Marquard-Moellenstedt, T.; Specht, M. H<sub>2</sub> rich product gas by steam gasification of biomass with in situ CO<sub>2</sub> absorption in a dual fluidized bed system of 8 MW fuel input. *Fuel Process. Technol.* **2009**, *90*, 914–921.
- (22) Specht, M.; Brellochs, J.; Frick, V.; Steiert, S.; Stürmer, B.; Zuberbühler, U. *AER-Technology and SNG from AER-Gas*. Presented at *Gasification 2010—Feedstock, Pretreatment and Bed Material*, Gothenburg, Sweden, 2010.
- (23) Shen, L.; Zheng, M.; Xiao, J.; Zhang, H.; Xiao, R. Chemical looping combustion of coal in interconnected fluidized beds. *Sci. China, Ser. E: Technol. Sci.* **2007**, *50*, 230–240.
- (24) Shen, L.; Wu, J.; Xiao, J.; Song, Q.; Xiao, R. Chemical-Looping Combustion of Biomass in a 10 kW<sub>th</sub> Reactor with Iron Oxide as an Oxygen Carrier. *Energy Fuels* **2009**, *23*, 2498–2505.
- (25) Grasa, G. S.; Abanades, J. C. CO<sub>2</sub> Capture capacity of CaO in long series of carbonation/calcination cycles. *Ind. Eng. Chem. Res.* **2006**, *45*, 8846–8851.
- (26) Abanades, J. C.; Anthony, E. J.; Wang, J.; Oakey, J. E. Fluidized bed combustion systems integrating CO<sub>2</sub> capture with CaO. *Environ. Sci. Technol.* **2005**, *39*, 2861–2866.
- (27) Pfeifer, C.; Puchner, B.; Hofbauer, H. Comparison of dual fluidized bed steam gasification of biomass with and without selective transport of CO<sub>2</sub>. *Chem. Eng. Sci.* **2009**, *64*, 5073–5083.
- (28) Song, G.; Chen, L.; Xiao, J.; Shen, L. Exergy evaluation of biomass steam gasification via interconnected fluidized beds. *Int. J. Energy Res.* DOI: 10.1002/er.2987.
- (29) Van Ree, R.; Oudhuis, A. B. J.; Faaij, A. Modelling of a biomass-integrated-gasifier/combined-cycle (BIG-CC) system with the flow-sheet simulation program Aspen-plus. Report No. ECN-C-95-041, Department of Science Technology and Society, Utrecht University: Utrecht, The Netherlands, 1995.
- (30) Wen, F. *Introduction to modern power plant* (in Chin.), 2nd Edition; China Electric Power Press; Beijing, 2008.
- (31) Lampert, K.; Ziebig, A. Comparative analysis of energy requirements of CO<sub>2</sub> removal from metallurgical fuel gases. *Energy* **2007**, *32*, 521–527.
- (32) Szargut, J.; Morris, D. R.; Steward, F. R. *Exergy Analysis of Thermal, Chemical and Metallurgical Processes*; Hemisphere Publishing Corporation: New York, 1988.
- (33) Szargut, J.; Valero, A.; Stanek, W.; Valero, A. Towards an international legal reference environment. *Proceedings of ECOS 2005*, Trondheim, Norway, 2005; pp 409–417.
- (34) Song, G.; Xiao, J.; Zhao, H.; Shen, L. A unified correlation for estimating specific chemical exergy of solid and liquid fuels. *Energy* **2012**, *40*, 164–173.
- (35) Song, G.; Feng, F.; Xiao, J.; Shen, L. Technical assessment of synthetic natural gas (SNG) production from agriculture residuals. *J. Thermal Sci.* **2013**, *22* (4), 359–365.